marine drugs

MDPI

Article

Hydantoanabaenopeptins from Lake Kinneret *Microcystis* Bloom, Isolation, and Structure Elucidation of the Possible Intermediates in the Anabaenopeptins Biosynthesis

Shira Weisthal Algor [1], Assaf Sukenik [2] and Shmuel Carmeli [1,*]

[1] Raymond and Beverly Sackler Faculty of Exact Sciences, School of Chemistry, Tel Aviv University, Tel Aviv 69978, Israel; shiraw1@mail.tau.ac.il
[2] The Yigal Allon Kinneret Limnological Laboratory, Israel Oceanographic & Limnological Research Institute, Migdal 49500, Israel; assaf@ocean.org.il
* Correspondence: carmeli@tauex.tau.ac.il; Tel.: +972-54-3117290

Abstract: Anabaenopeptins are common metabolites of cyanobacteria. In the course of reisolation of the known aeruginosins KT608A and KT608B for bioassay studies, we noticed the presence of some unknown anabaenopeptins in the extract of a *Microcystis* cell mass collected during the 2016 spring bloom event in Lake Kinneret, Israel. The ^{1}H NMR spectra of some of these compounds presented a significant difference in the appearance of the ureido bridge protons, and their molecular masses did not match any one of the 152 known anabaenopeptins. Analyses of the 1D and 2D NMR, HRMS, and MS/MS spectra of the new compounds revealed their structures as the hydantoin derivatives of anabaenopeptins A, B, F, and ^{1}[Dht]-anabaenopeptin A and oscillamide Y (**1**, **2**, **3**, **6**, and **4**, respectively) and a new anabaenopeptin, ^{1}[Dht]-anabaenopeptin A (**5**). The known anabaenopeptins A, B, and F and oscillamide Y (**7**, **8**, **9,** and **10**, respectively) were present in the extract as well. We propose that **1**–**4** and **6** are the possible missing intermediates in the previously proposed partial biosynthesis route to the anabaenopeptins. Compounds **1**–**6** were tested for inhibition of the serine proteases trypsin and chymotrypsin and found inactive at a final concentration of ca. 54 μM.

Keywords: cyanobacteria; *Microcystis*; anabaenopeptin; cyclopeptide; hydantoin derivatives

Citation: Weisthal Algor, S.; Sukenik, A.; Carmeli, S. Hydantoanabaenopeptins from Lake Kinneret *Microcystis* Bloom, Isolation, and Structure Elucidation of the Possible Intermediates in the Anabaenopeptins Biosynthesis. *Mar. Drugs* **2023**, *21*, 401. https://doi.org/10.3390/md21070401

Academic Editor: Bill J. Baker

Received: 25 May 2023
Revised: 9 July 2023
Accepted: 11 July 2023
Published: 13 July 2023

1. Introduction

Anabaenopeptins are common metabolites of cyanobacteria, especially water-bloom-forming genera, but have been isolated from terrestrial and marine (*Anabeana* sp. and *Nudularia spumigena*) cyanobacteria and marine sponges (*Theonella* spp. and *Melophlus* sp.) as well [1]. They are nonribosomally synthesized cyclic-peptides that, in cyanobacteria, are composed of five variable L-amino acids and a conserved D-lysine. Their general structure is ^{1}X-CO-[^{2}Lys-^{3}X-^{4}X-*N*Me-^{5}X-^{6}X], where their macrocycle is derived from the cyclization of Lys-e-NH_2 to the carboxyl of the sixth amino acid. The Lys-a-amine is connected through an ureido bridge to the a-amine of the first amino acid. The chemical shifts of the latter urea-amide protons are distinctive and commonly allocated between 6 and 7 ppm in the ^{1}H NMR in DMSO-d_6. The latest report sums the number of known anabaenopeptins to 152, many of which resulted from LC–MS/MS studies, which, according to our findings, sometimes fail to report the correct structure of the compounds (see below) [2]. The anabaenopeptins were reported to exhibit inhibitory activity toward serine proteases, carboxypeptidases, and phosphatases [1]. Their biosynthesis was studied by the analyses of gene clusters isolated from different strains of cyanobacteria, *Anabaena* sp., *Nodularia spumigena* [3], *Nostoc punctiforme* [4], *Sphaerospermopsis torques-reginae* [5], *Planktothrix agardhii* [6], and *Snowella* sp. [7], and three strains of *Microcystis aeruginosa* [8,9], all showing great similarity. However, no explanation was given in these studies to the transformation of the amide bond between the *N*-terminal amino acid and ^{2}Lys to an ureido bridge between the a-amines of the latter

amino acids. In the process of isolating the known aeruginosins KT608A and KT608B for bioassay studies, from the 2016 spring *Microcystis* bloom (dominant by the *Microcystis aeruginosa* strain marked Mic B due to its dominant pigmentation, brown color) [10,11], we isolated small quantities of 10 anabaenopeptins (**1**–**10**), 6 of which (**1**–**6**) turned to be novel, and their structure elucidation is described herein (Figure 1). Only one of the compounds, **5**, was identified as a new anabaenopeptin derivative. The other five compounds, **1**–**4** and **6**, presented an unusual ^{1}H NMR spectrum for anabaenopeptins, where the typical ureido bridge protons were missing from the spectrum, but the distinctive *N*Me signal was present. Four of the latter five compounds presented doubling of some proton and carbon signals in their ^{1}H and ^{13}C NMR spectra. A full structure elucidation of these compounds revealed that they share a unique hydantoin moiety composed of a urea-type CO, a carboxyamide, a Ca and a-NH of a varied amino acid, and the a-N of the lysine residue. Based on the structure of these compounds, we propose four alternative biosynthetic routes to the anabaenopeptins, which are based on the partial biosynthetic route proposed, established by genome mining, in the past [3–9].

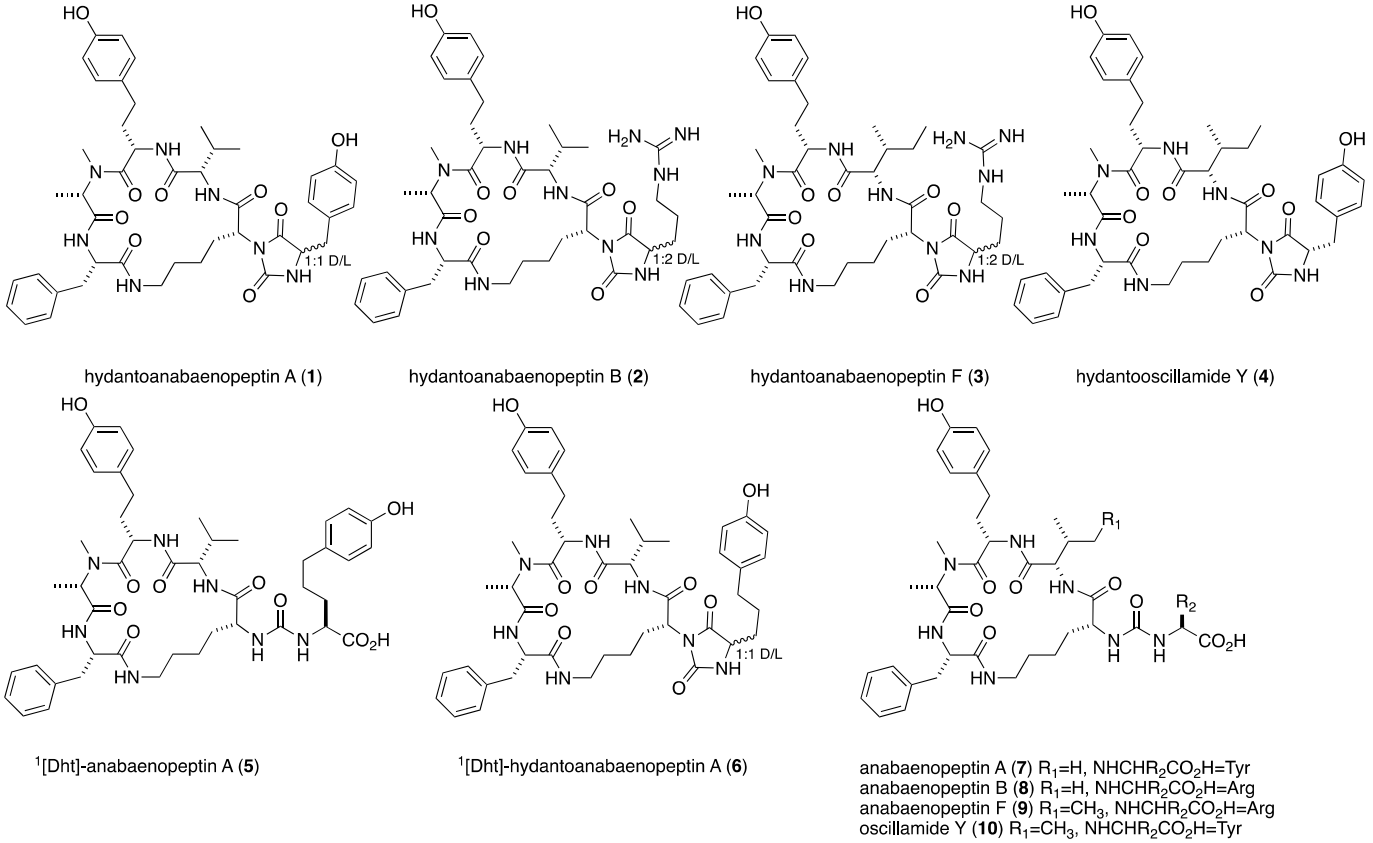

Figure 1. Anabaenopeptins isolated from *Microcystis* biomass collected from Lake Kinneret during the 2016 winter-spring bloom, TAU collection # IL-444.

2. Results and Discussion

Hydantoanabaenopeptin A (**1**) presented a molecular ion (negative HR ESI MS, [M-H]$^{-}$) at *m*/*z* 824.4016 corresponding to the molecular formula $C_{44}H_{55}N_7O_9$ and 21 degrees of unsaturation. The IR spectrum of **1** presented stretching bands at 3274 (amide-NH), 1766 (CO), 1710 (CO), 1640 (amide-CO), and 1592 (aromatic-C=C) cm^{-1}, of which those at 1766 (C-4) and 1710 (C-2) cm^{-1} are characteristic of five-membered carbonyls of hydantoin [12]. The ^{1}H NMR spectrum of **1** in DMSO-d_6 (see Table 1 for the signals of the major signals and Figure S1 and Table S1 in supporting material for both major and minor signals) presented doubling of signals at a ratio of 2:1 of all of the amide protons and a-protons and many other signals in the spectrum. In the ^{13}C NMR spectrum of **1**, most of the carbonyls and

α-carbons were doubled at a ratio of 2:1, as well as few of the amino acid side-chain carbons (Figure S2). Analysis of the 2D NMR data (COSY, TOCSY, HSQC, and HMBC) of **1** in DMSO-d_6 revealed the presence of the following amino acid residues: Phe, *N*Me-Ala, Hty, Val, Tyr, and a trisubstituted Lys (in which the expected a-amide proton was missing) and a urea-type carbonyl, similar to the one incorporated in the anabaenopeptin skeleton (Table S1) [13,14]. The latter composition of amino acids resembled those of anabaenopeptin A (**7**) [13]. The assembly of the amino acids by HMBC and ROESY correlations revealed the same amino acid sequence, cyclo-(Phe-*N*MeAla-Hty-Val-Lys-ε-NH)-, as in anabaenopeptin A, for the macrocycle of **1**. The carbon chemical shifts of Lys C-1 to C-4 were different from the regular chemical shifts of these carbons in the anabaenopeptins [13]. Lys C-1 and C-3 were up-field-shifted (γ substitution effect), while C-2 and C-4 were down-field-shifted (β and δ substitution effects, respectively), in accordance with an extra substitution of the α-nitrogen of Lys. The diastereotopic character of Lys β-protons (Lys-3a and Lys-3b) appears to be much more pronounced in **1** (δ_H 2.12 and 0.84, respectively) than in anabaenopeptin A (**7**, δ_H 1.28 and 1.18, respectively). The chemical shifts of the carbons of the substituted Tyr residue of **1** presented some differences from those of anabaenopeptin A (**7**) [13]. Although Tyr-CO (Tyr-1) and the ureido-CO presented chemical shifts similar to those of anabaenopeptin A (**7**), Tyr-C-2 to C-4 presented significant differences, with C-2 up-field-shifted and C-3 and C-4 down-field-shifted relative to those of anabaenopeptin A (**7**) [13]. The chemical shifts of Tyr-H-2 (Dd 0.5 ppm) and especially that of Tyr-NH (Dd 2.6 ppm) were significantly down-field-shifted relative to the latter in anabaenopeptin A (**7**). In the HMBC spectrum, Tyr-CO presented correlations with Lys-H-2, Tyr-H-2, Tyr-NH, and Tyr-H-3a, while "urea"-CO presented correlations with Lys-H-2, Tyr-H-2, and Tyr-NH, suggesting an extra hydantoin-type cycle for **1**, in accordance with the 21 degrees of unsaturation. This finding was supported by the strong fragment ion in the MS/MS spectrum of **1**, m/z 621.3406 ($[C_{34}H_{47}N_5O_6]^+$), which resulted from the fragmentation of the C–N bond between Lys-C-2 and Lys-nitrogen (which is part of the hydantoin moiety, Figure S10). The strongest fragment ion in the spectrum, m/z 649.3352 (B in Scheme 1, $[C_{35}H_{47}N_5O_7]^+$), for which we suggest a migration process of ureido-CO to Lys-C-2, and the strong $M+H^+$-CO fragment ion at m/z 798.4196 are, as well, in accordance with the proposed hydantoin moiety. We assumed that the doubling in the NMR spectra of **1** resulted from the restricted rotation of the hydantoin moiety around the Lys C–N bond. However, when we tried to confirm it by running the ^{1}H NMR spectrum at an elevated temperature, the ratio of the doubled signals changed to 1:1 when the temperature reached 390 °K, and the ratio remained unchanged after lowering the temperature back to room temperature, suggesting that the doubling in the spectra is a result of the epimerization of a chiral center of one of the amino acids in **1**. Application of Marfey's method [15] coupled with HR ESI LCMS established the absolute configuration of the amino acids as L-NMeAla, L-Hty, L-Phe, L-Val, D-Lys, and 1:1 D,L-Tyr (Figure S11). We suspect that the tyrosine epimerization occurs due to the easy keto/enol tautomerism of the hydantoin moiety during the compound separation [16]. Based on these arguments, structure **1** was proposed for hydantoanabaenopeptin A.

Table 1. ^{1}H and ^{13}C NMR data of hydantoanabaenopeptins **1**–**4** in DMSO-d_6 [a].

Compounds	**1**		**2**		**3**		**4**	
Position	δ_C	δ_H	δ_C	δ_H	δ_C	δ_H	δ_C	δ_H
Tyr/Arg-1	174.1, C		174.6, C		174.8, C		174.1, C	
Tyr/Arg-2	57.0, CH	4.34	55.9, CH	4.17	56.0, CH	4.14	57.0, CH	4.35
Tyr/Arg-2-NH		8.55		8.69		8.74		8.55
Tyr/Arg-3a	35.5, CH_2	2.89	28.8, CH_2	1.73	28.9, CH_2	1.74	35.5, CH_2	2.88
Tyr/Arg-3b		2.82		1.52		1.52		2.82
Tyr/Arg-4	124.3, C		24.2, CH_2	1.54 1.45	24.2, CH_2	1.50 1.42	124.4, C	

Table 1. *Cont.*

Compounds	1		2		3		4	
Position	δ_C	δ_H	δ_C	δ_H	δ_C	δ_H	δ_C	δ_H
Tyr-5,5′/Arg-5	130.9, CH	6.88	40.1, CH_2	3.04	40.0, CH_2	3.05	130.9, CH	6.89
Tyr-6,6′/Arg-6 -NH	115.0, CH	6.61		8.86		9.05	115.0, CH	6.61
Tyr/Arg-7	156.7, C		156.7, C		157.8, C		156.6, C	
Arg-7-NH_2, NH_2^+				8.43		8.03		
CO	156.4, C		156.9, C		156.9, C		156.4, C	
Lys-1	167.9, C		168.2, C		168.4, C		168.1, C	
Lys-2	56.3, CH	4.08	56.4, CH	4.30	56.5, CH	4.32	56.4, CH	4.08
Lys-3a	29.3, CH_2	2.12	29.6, CH_2	2.40	29.6, CH_2	2.39	29.3, CH_2	2.10
Lys-3b		0.84		1.45		1.45		0.86
Lys-4a	22.9, CH_2	1.48	23.1, CH_2	1.51	23.1, CH_2	1.45	22.8, CH_2	1.36
Lys-4b		1.37		1.18		1.19		1.00
Lys-5a	28.6, CH_2	1.37	28.5, CH_2	1.50	28.3, CH_2	1.51	28.3, CH_2	1.39
Lys-5b		1.30		1.40		1.46		1.34
Lys-6a	38.4, CH_2	3.54	38.5, CH_2	3.55	38.6, CH_2	3.53	38.5, CH_2	3.53
Lys-6b		2.63		2.66		2.66		2.63
Lys-6-NH		7.41		7.43		7.46		7.41
Val/Ile-1	172.4, C		172.4, C		172.5, C		172.5, C	
Val/Ile-2	57.9, CH	3.98	57.9, CH	4.09	56.4, CH	4.26	56.4, CH	4.15
Val/Ile-2-NH		7.76		7.87		7.89		7.82
Val/Ile-3	30.4, CH	1.96	30.5, CH	2.03	36.7, CH	1.85	36.7, CH	1.79
Val/Ile-4	19.1, CH_3	0.96	19.1, CH_3	1.00	25.6, CH_2	1.53	25.5, CH_2	1.48
						1.15		1.08
Val/Ile-5	18.9, CH_3	0.88	18.9, CH_3	0.94	11.8, CH_3	0.89	11.8, CH_3	0.88
Ile-6					14.8, CH_3	0.89	14.8, CH_3	0.84
Hty-1	171.2, C		171.1, C		171.1, C		171.1, C	
Hty-2	48.9, CH	4.74	48.9, CH	4.77	49.0, CH	4.77	49.0, CH	4.74
Hty-2-NH		8.97		8.98		8.98		8.92
Hty-3a	33.5, CH_2	1.85	33.4, CH_2	1.85	33.4, CH_2	1.85	33.4, CH_2	1.85
Hty-3b		1.73		1.74		1.74		1.72
Hty-4a	30.7, CH_2	2.60	30.7, CH_2	2.61	30.8, CH_2	2.62	30.7, CH_2	2.59
Hty-4b		2.40		2.42		2.42		2.40
Hty-5	131.0, C		131.1, C		131.0, C		131.1, C	
Hty-6,6′	129.2, CH	6.98	129.2, CH	6.98	129.1, CH	6.98	129.2, CH	6.97
Hty-7,7′	115.3, CH	6.66	115.3, CH	6.66	115.4, CH	6.66	115.3, CH	6.65
Hty-8	155.9, C		155.8, C		155.9, C		155.8, C	
NMe-Ala-1	170.0, C		170.0, C		170.0, C		170.0, C	
NMe-Ala-2	54.5, CH	4.85	54.6, CH	4.87	54.6, CH	4.88	54.5, CH	4.85
NMe-Ala-3	14.1, CH_3	1.05	14.1, CH_3	1.07	14.1, CH_3	1.07	14.1, CH_3	1.06
NMe-Ala-Me	27.2, CH_3	1.78	27.3, CH_3	1.79	27.3, CH_3	1.81	27.3, CH_3	1.79
Phe-1	170.9, C		171.2, C		171.3, C		171.2, C	
Phe-2	55.1, CH	4.34	55.1, CH	4.36	55.2, CH	4.35	55.2, CH	4.35
Phe-2-NH		8.69		8.70		8.65		8.65
Phe-3a	37.7, CH_2	3.23	37.7, CH_2	3.23	37.7, CH_2	3.23	37.7, CH_2	3.24
Phe-3b		2.81		2.83		2.84		2.82
Phe-4	138.5, C		138.4, C		138.5, C		138.5, C	
Phe-5,5′	129.1, CH	7.06	129.0, CH	7.07	129.1, CH	7.07	129.1, CH	7.07
Phe-6,6′	128.5, CH	7.19	128.5, CH	7.19	128.4, CH	7.19	128.4, CH	7.19
Phe-7	126.3, CH	7.14	126.3, CH	7.14	126.3, CH	7.14	126.3, CH	7.16

[a] 500 MHz for ^1H and 125 MHz for ^{13}C, data of the major components.

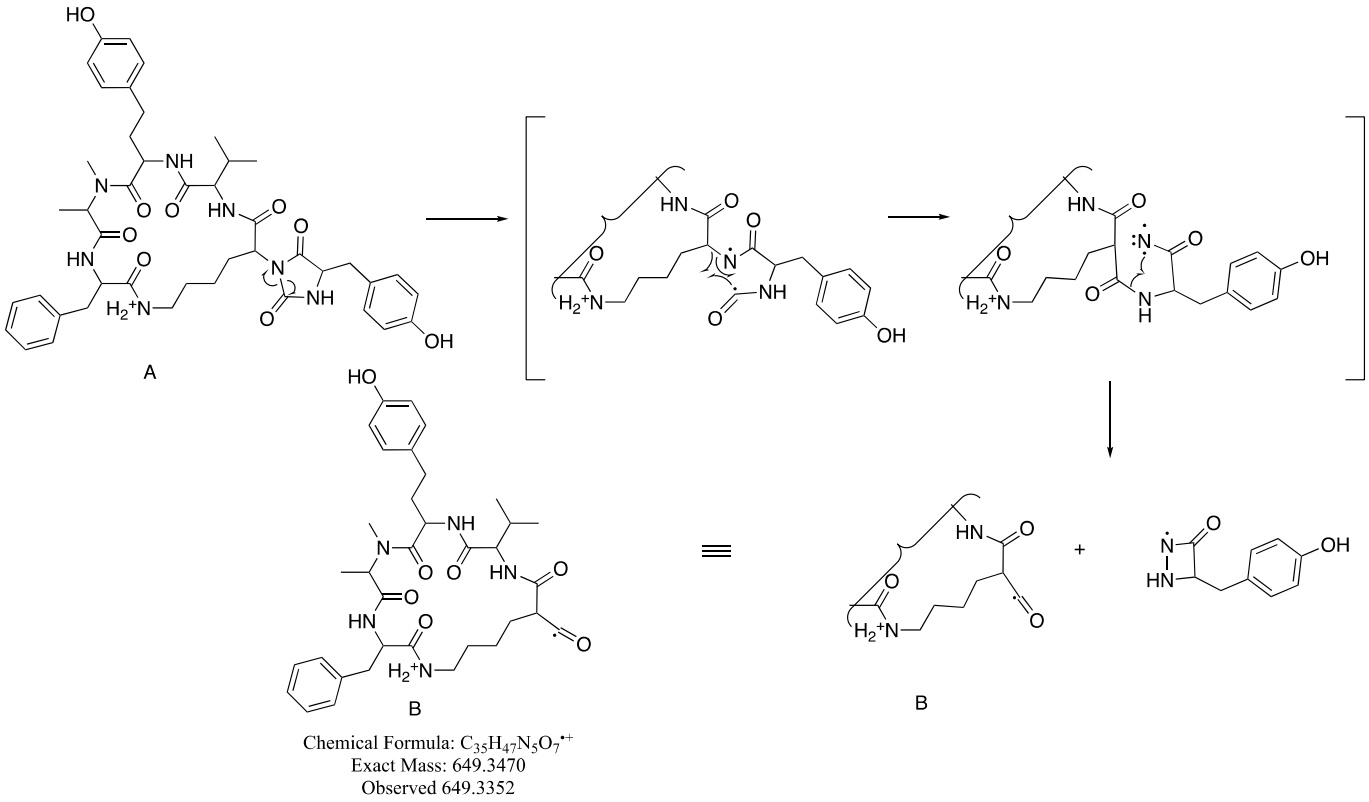

Scheme 1. Proposed mechanism of the migration process of the ureido carbonyl in the mass spectrometer.

Hydantoanabaenopeptin B (**2**) presented a negative HR ESI MS molecular ion, $[M-H]^-$ ion, at m/z 817.4361 corresponding to the molecular formula $C_{42}H_{58}N_{10}O_8$ and 18 degrees of unsaturation. Like for **1**, the ^1H and ^{13}C NMR spectra of **2** presented doubling at a ratio of ca. 1:1 of all of the amide protons, two carbonyl carbons, two a-carbons, and few side-chain carbons (see Figures S12 and S13, Tables 1 and S2). Analysis of the 2D NMR data (COSY, TOCSY, HSQC, HMBC) of **2** revealed that it is composed of the amino acids Phe, *N*MeAla, Hty, Val, Lys, and Arg, where the last two amino acids presented the most pronounced doubling of proton and carbon signals (Table S2). The amino acid composition of **2** was thus found to be identical with those of anabaenopeptin B (**8**) [13]. Based on the HMBC and NOE correlations (Table S2), the structure of **2** was assigned to be the hydantoin derivative of anabaenopeptin B. The proposed structure was supported by the MS/MS fragment ion at m/z 200.1147 ($[C_7H_{14}N_5O_2]^+$), which derived from the cleavage of the Lys C–N bond and the preferred allocation of the positive charge on the arginine moiety, and the strong $M+H^+$-CO fragment ion at m/z 791.4575 (Figure S21). As for **1**, the Lys β-protons presented a pronounced diastereotopic difference. The application of Marfey's method [15], coupled with HR ESI LCMS, established the absolute configuration of the amino acids as L-NMeAla, L-Hty, L-Phe, L-Val, D-Lys, and 1:2 D,L-Tyr (Figure S22), confirming the structure of hydantoanabaenopeptin B as **2**.

Hydantoanabaenopeptin F (**3**) presented a positive HR ESI MS molecular cluster ion, $M+H^+$, at m/z 833.4688 corresponding to the molecular formula $C_{42}H_{60}N_{10}O_8$ and 18 degrees of unsaturation. The ^1H and ^{13}C NMR spectra of **3** presented doubling at a ratio of ca. 1:1 of all of the amide protons, three carbonyl carbons, three α-carbons, and a few side-chain carbons (see Figures S23 and S24, Tables 1 and S3), similar to those of **2**. Analysis of the 2D NMR data (COSY, TOCSY, HSQC, HMBC) of **3** revealed that it is composed of the amino acids Phe, *N*MeAla, Hty, Ile, Lys, and Arg, where the last three amino acids presented the most pronounced doubling of proton and carbon signals (Figures S23 and S24 and Table S3). The sequence of the amino acids in the peptide, Phe, *N*MeAla, Hty,

Ile, Lys, and Arg, was elucidated based on the correlations from the HMBC and ROESY 2D spectra of **3** (Table S3) to be identical with that of anabaenopeptin F (**9**) [14] except of the extra correlations of both Lys-H-2 and Arg-2-NH with Arg-CO and ureido-CO, which suggest the closure of a hydantoin moiety similar to that of **2**. The isoleucine moiety was identified by its characteristic ^{1}H and ^{13}C chemical shifts (5-Me: δ_H 0.89 t, δ_C 11.8 CH_3: 6-Me, δ_H 0.89 d, δ_C 14.8 CH_3) to be *allo*-isoleucine in accordance with the chemical shifts of L-*allo*-isoleucine in ferintoic acid A [17] (5-Me: δ_H 0.88 t, δ_C 11.5 CH_3: 6-Me, δ_H 0.87 d, δ_C 14.9 CH_3) and different from those of L-Ile (5-Me: δ_H 0.73–0.82 t, δ_C 10.3–10.8 CH_3: 6-Me, δ_H 0.88–1.00 d, δ_C 14.9–15.5 CH_3) in anabaenopeptin F [14], lyngbyaureidamide A [18], and schizopeptin 791 [19] and those of D-Ile (5-Me: δ_H 0.88 t, δ_C 12.3 CH_3: 6-Me, δ_H 0.85 d, δ_C 16.5 CH_3) in mozamide B [20]. The proposed structure was supported by the MS/MS fragment at m/z 200.1140 ($[C_7H_{14}N_5O_2]^+$), which derived from the cleavage of the Lys C–N bond and the preferred allocation of the positive charge on the arginine moiety, the complementary (-C_2H_3) strong fragment ion at m/z 611.2669 (Figure S32), and the strong M+H$^+$-CO fragment ion at m/z 805.4730 (Figure S32). The application of Marfey's method [15] in conjugation with HR ESI LCMS established the absolute configuration of the amino acids as L-NMeAla, L-Hty, L-Phe, L-*allo*Ile, D-Lys, and 1:2 D,L-Arg (Figure S33), verifying the structure of hydantoanabaenopeptin F as **3**.

Hydanto-oscillamide Y (**4**) gave a negative HR ESI MS molecular ion at m/z 838.4143 corresponding to a molecular formula of $C_{45}H_{57}N_7O_9$ and 21 degrees of unsaturation. The ^{1}H and ^{13}C NMR spectra of **4** (Table 1, Figures S34 and S35) presented, in contrast to **1**–**3**, a single rotamer; however, the chemical shifts of the protons and carbons of the Lys and the Tyr moieties were shifted similarly to those of **1**. Analysis of the 2D NMR data (COSY, TOCSY, ROESY, HSQC, HMBC, Table S4) of **4** revealed that it is composed of the amino acids Phe, *N*MeAla, Hty, Ile, Lys, and Tyr as in oscillamide Y (**10**) [21] and established its structure as hydanto-oscillamide Y. The latter structure was supported by a strong fragment ion in the MS/MS spectrum of **4**, m/z 635.3560 ($[C_{35}H_{49}N_5O_6]^+$), which resulted from the fragmentation of the C–N bond between Lys-C-2 and the nitrogen of the hydantoin moiety (Figure S43), and the fragment ion at m/z 663.3527 ($[C_{36}H_{49}N_5O_7]^+$), in accordance with the fragmentations of **1**. The application of Marfey's method [15] in conjugation with HR ESI LCMS established the absolute configuration of the amino acids as L-NMeAla, L-Hty, L-Phe, L-*allo*Ile, D-Lys, and L-Tyr (Figure S44), confirming the structure of hydanto-oscillamide Y as **4**.

^{1}[Dht]-anabaenopeptin A (**5**) presented a positive HR ESI MS protonated cluster ion at m/z 872.4572 corresponding to a molecular formula of $C_{46}H_{61}N_7O_{10}$ and 20 degrees of unsaturation. The latter molecular ion and molecular formula suggest 28 mass units and C_2H_4 difference, respectively, from those of anabaenopeptin A. The ^{1}H NMR spectrum of **5** in DMSO-d_6 (Table 2, Figure S45) presented a typical anabaenopeptin spectrum [13] with the ureido bridge amide protons appearing as doublets at 6.48 and 6.27 ppm, 13 aromatic protons corresponding to a phenyl and two *p*-phenol rings, a singlet *N*-Me group at 1.76 ppm, and three doublet methyl groups at 1.05, 1.02, and 0.92 ppm, suggesting that **5** contains *N*-MeAla and valine residues. Analysis of the 2D NMR data (COSY, TOCSY, ROESY, HSQC, HMBC, Table S5) of **5** revealed that the five amino acids of the cycle in it are identical to those of anabaenopeptin A, Phe, *N*MeAla, Hty, Val, and Lys, while the sixth amino acid turned to be an amino acid first described in the anabaenopeptins, which we named dihomotyrosine (Dht) based on the analogy to the known biosynthesis of homophenylalanine and homotyrosine in cyanobacteria [22]. The 2D spectra failed to assign the two carboxy carbons resonating at 174.6 and 171.2 ppm, which were assigned by comparison with those of anabaenopeptin A [13], as Dht-C-1 and Phe-C-1, respectively. The structure of Dht was supported by the fragment ions at m/z 210.1109 ($[C_{11}H_{16}NO_3]^+$) and 663.3516 ($[C_{35}H_{45}N_6O_7]^+$) in the HR ESI MS/MS of **5** (Figure S54). Dihomotyrosine is homologous to PNV (5-phenylnorvaline) previously described in anabaenopeptins SA4 and SA7 [23]. The sequence of the amino acids in **5** was established as Dht-CO-cyclo-[Lys-Val-Hty-*N*MeAla-Phe] based of the HMBC correlations of Phe-NH with *N*MeAla-CO, *N*MeAla-

H-2, and -*N*-Me with Hty-CO, Hty-NH with Val-CO, and the NOE correlations between Dth-NH and Lys-2-NH, Lys-6-NH and Phe-NH, Phe-NH and *N*MeAla-H-2, *N*MeAla-H-2 and Hty-NH, and Hty-H-2 and Val-H-2, leaving only the connection of Val-NH and Lys-CO unproved. However, the strong HR ESI MS/MS fragment ions at *m*/*z* 775.1253, 695.3779, and 637.3714 support the cyclic structure of **5** (Figure S54). The application of Marfey's method [15] in conjunction with HR ESI LCMS established the absolute configuration of the amino acids as L-NMeAla, L-Hty, L-Phe, L-Val, D-Lys, and L-Dht (Figure S55), establishing the structure of [1][Dht]-anabaenopeptin A as **5**.

Table 2. ^{1}H and ^{13}C NMR data of compounds **5** and **6** in DMSO-d_6 [a].

Compounds	**5**		**6**	
Position	**δ_C**	**δ_H**	**δ_C**	**δ_H**
Dht-1	174.6, C		174.0, C	
Dht-2	53.3, CH	3.91, m	56.2, CH	4.15, m
Dht-2-NH		6.27, brd		8.61, brs
Dht-3a	32.3, CH_2	1.61, m	30.8, CH_2	1.66, m
Dht-3b		1.50, m		1.50, m
Dht-4a	27.7, CH_2	1.48, m	28.9, CH_2	1.48, m
Dht-4b		1.45, m		1.45, m
Dht-5	34.4, CH_2	2.40, m	34.0, CH_2	2.42, m
Dht-6	132.4, C		131.6, C	
Dht-7,7′	129.2, CH	6.92, d	129.3, CH	6.92, d
Dht-8,8′	115.2, CH	6.63, d	115.2, CH	6.65, d
Dht-9	155.4, C		155.9, C	
CO	157.4, C		156.9, C	
Lys-1	172.7, C		168.4, C	
Lys-2	55.0, CH	3.91, ddd	56.5, CH	4.31, m
Lys-2-NH		6.48, brd		-
Lys-3	32.1, CH_2	1.60, m	29.6, CH_2,	2.39, m
				1.44, m
Lys-4a	20.6, CH_3	1.28, m	23.1, CH_2	1.45, m
Lys-4b		1.16, m		1.17, m
Lys-5	28.3, CH_2	1.41, m	28.6, CH_2	1.48, m
				1.38, m
Lys-6a	38.5, CH_2	3.56, m	38.5, CH_2	3.53, m
Lys-6b		2.78, m		2.65, m
Lys-6-NH		7.14, m		7.43, t
Val-1	172.9, C		172.4, C	
Val-2	58.4, CH	3.88, dd	57.9, CH	4.08, t
Val-2-NH		7.06, m		7.88, d
Val-3	30.2, CH_2	1.95, dqq	30.5, CH	2.01, m
Val-4	19.6, CH_3	0.92, d	19.2, CH_3	0.99, d
Val-5	19.1, CH_3	1.02, d	18.8, CH_3	0.92, d
Hty-1	171.1, C		171.2, C	
Hty-2	48.9, CH	4.71, dt	49.0, CH	4.77, m
Hty-2-NH		8.92, d		8.96, brs
Hty-3a	33.5, CH_2	1.85, m	33.4, CH_2	1.85, m
Hty-3b		1.70, m		1.72, m
Hty-4a	30.7, CH_2	2.62, m	30.7, CH_2	2.60, m
Hty-4b		2.41, m		2.40, m
Hty-5	131.2, C		131.0, C	
Hty-6,6′	129.3, CH	7.00, d	129.2, CH	6.98, d
Hty-7,7′	115.4, CH	6.65, d	115.4, CH	6.66, d
Hty-8	155.8, C		155.7, C	
NMe-Ala-1	170.1, C		170.0, C	
NMe-Ala-2	54.5, CH	4.77, q	54.6, CH	4.87, q
NMe-Ala-3	14.1, CH_3	1.05, d	14.1, CH_3	1.06, d
NMe-Ala-Me	27.3, CH_3	1.76, s	27.3, CH_3	1.79, s
Phe-1	171.2, C		171.1, C	

Table 2. *Cont.*

Compounds	5		6	
Position	**δ_C**	**δ_H**	**δ_C**	**δ_H**
Phe-2	55.2, CH	4.36, ddd	55.2, CH	4.35, ddd
Phe-2-NH		8.68, d		8.69, d
Phe-3a	37.7, CH_2	3.30, m	37.7, CH_2	3.23, m
Phe-3b		2.77, dd		2.81, dd
Phe-4	138.5, C		138.4, C	
Phe-5,5′	129.1, CH	7.05, d	129.1, CH	7.07, d
Phe-6,6′	128.5, CH	7.18, dd	128.5, CH	7.19, t
Phe-7	126.3, CH	7.13, t	126.3, CH	7.14, t

[a] 500 MHz for ^{1}H and 125 MHz for ^{13}C, data of only the major component of **6**.

The anabaenopeptin E [14] structure was established based on analysis of its NMR and MS data to contain 7-methylhomotyrosine at the fourth position. However, MS/MS studies on bloom material or compounds accumulated in animal organs cannot distinguish 7-methylhomotyrosine (MeHty) from dihomotyrosine (due to the identical mass and molecular formula) unless a dipper study based on MS^n is utilized. We believe that many of the publications in which MS/MS studies (i.e., Riba et al. [24]) were used to report the structure of cyanobacteria metabolites erroneously report the presence of MeHty instead of Dht.

^{1}[Dht]-hydantoanabaenopeptin A (**6**) exhibited a positive HR ESI MS protonated cluster ion at m/z 854.4464 corresponding to the molecular formula $C_{46}H_{60}N_7O_9$ and 21 degrees of unsaturation. The ^{1}H and ^{13}C NMR spectra of **6** (Figure S56 and S67) presented a 1:1 signal doubling as in **2**, while the chemical shifts of the protons and carbons of the Lys were shifted similarly to those of **1**. Analysis of the 2D NMR data (COSY, TOCSY, ROESY, HSQC, HMBC, Table S6) of **6** revealed that it is composed of the same amino acids as **5**—Phe, NMeAla, Hty, Val, Lys, and Dht—and established its structure as ^{1}[Dht]-hydantoanabaenopeptin A. The assignment of Dht-C-1 was suggested based on its HMBC correlation with Dht-NH and the NOE correlation of the latter with Dht-H-2. The HMBC correlations of Dht-H-2 and Lys-H-2 with urea-type-CO connected both acids and, in the absence of Lys-a-NH, suggested the hydantoin cycle. The connection of Lys-C-1 to Val-NH was suggested based on the HMBC correlation of Lys-H-2 with Lys-C-1 and the NOE of Val-NH with Lys-H-3a. HMBC correlations of Val-C-1 with Val-H-2 and Hty-NH and of NMeAla-C-1 with NMeAla-H-2 and Phe-NH suggested the connection of the latter amino acids. NMeAla-H-2 and NMe presented correlations with the carboxyl carbon resonating at 171.2 ppm, and NMeAla-H-2 presented NOE correlation with Hty-H-2, assigning the latter carbon as Hty-C-1 and confirming the connection between NMe-Ala and Hty. Lys-e-NH presented HMBC correlation with the carboxyl carbon resonating at 171.1 ppm and NOE correlation with Phe-NH, thus confirming their connection and the assignment of Phe-C-1. The structure of **6** was supported by the characteristic MS/MS fragmentations (as in **1** and **4**): m/z 826.4515 ($M+H^+$-CO, $[C_{45}H_{60}N_7O_8]^+$), 649.3719 ($[C_{35}H_{47}N_5O_7]^+$), and 622.3248 ($[C_{34}H_{48}N_5O_6]^+$) (Figure S65), affirming the hydanto-Dht-[Lys-Val-Hty-NMeAla-Phe] structure of **6**. The absolute configuration of the amino acids of **6** was established by the application of Marfey's method [15] in conjunction with HR ESI LCMS to be L-NMeAla, L-Hty, L-Phe, L-Val, D-Lys, and D,L-Dht (Figure S66).

Compounds **1** and **4**–**6** were tested at concentrations of 55.1, 54.2, 53.3, and 53.3 μM, respectively, for the inhibition of the serine protease, chymotrypsin, and compounds **2** and **3** were tested at concentrations of 55.6 and 54.6 μM, respectively, for the inhibition of the serine protease and trypsin, but all were found nonactive at those concentrations.

The biosynthetic route proposed by genome mining and gene analyses [3–9] suggested a synthesis of a linear hexapeptide that contains in the second position a D-lysin, while the other five amino acids are varied L-amino acids of which the amino acid at the fifth position is *N*-methylated. The assembly of the six amino acids is followed by a release of the peptide from the enzyme and cyclization to the mature anabaenopeptin. However, no

explanation was given in these studies to the transformation of the amide bond between the *N*-terminal amino acid and the D-^{2}Lys to an ureido bridge between the a-amines of the latter two amino acids. Considering our proposal that the hydantoanabaenopeptins **1**–**4** and **6** are intermediates in the biosynthesis of **7**–**10** and **5**, respectively, several alternative routes are possible. The first one, route A in Scheme 2, suggests that the carboxylation of the *N*-terminus amine, cyclization to the hydantoin derivative, opening of the hydantoin to the ureido derivative, cleavage of the C-terminus thioester, and cyclization to the mature anabaenopeptin are mediated by the enzymes encoded in the last module of the biosynthetic cluster. Such a route would require the expression of at least one additional condensing enzyme in the last module of the gene cluster. The latter route is less reasonable due to the composition of enzymatic functions encoded in the last module of the biosynthetic cluster, C, A, T, and Te [3–9]. Routes B–D (Scheme 2) suggest loading of a presynthesized *N*-carboxy or *N*-carboxy-phosphate amino acid to the initial module of the biosynthetic cluster, explaining why no additional condensing enzyme is encoded in the biosynthetic cluster. The loading of a presynthesized *N*-carboxy-amino acid to the first adenylation domain of the anabaenopeptin biosynthetic enzyme cluster might explain its low specificity for certain amino acid [3–9], if the specificity is for the *N*-carboxy-moiety. Such specificity may lead to the production of a set of anabaenopeptins that differ in the starting unit but have a conserved sequence of amino acids in the ring, as in the case of the current study. In route B (Scheme 2), except for the loading of *N*-carboxy-amino acid, all of the other steps leading to the ureido bridge are facilitated by the last module of the biosynthetic cluster. In route C (Scheme 2), the hydantoin is proposed to be produced by the condensing enzyme encoded in the first module. The hydrolysis of the hydantoin to the ureido product is proposed to happen as the last step of the biosynthesis by the thioesterase (Te). The fourth possible route D suggests that both the cyclization to the hydantoin and its hydrolysis to the ureido moiety occur during the condensation process of lysine to the *N*-carboxy-amino acid. The hydantoin formation and opening might be catalyzed by a single enzyme of the cyclic amidohydrolase family (allantoinase, dihydropyrimidinase, dihydrooratase, hydantoinase, urease, and imidase) [25] that can reversibly catalyze the concession of *N*-carboxy-peptide to the hydantoin and its stereoselective hydrolysis to the ureido-bridge-containing peptide [26]. Alternatively, such conversion might be spontaneous in a similar fashion to the nonenzymatic isomerization of Asp in protein under physiological conditions. The latter isomerization proceeds through a succinimide intermediate and leads to racemization of the Asp and mixture of Asp and iso-linked-Asp, a total of four isomers [27]. However, the possibility that such transformation occurs spontaneously is low due to the stability toward hydrolysis of the hydantoin moiety of **1**–**4** and **6** in the isolation process (acidic aqueous solution) and even at 390 °K in DMSO-d_6. Thus, if such a process occurs in the biosynthesis of the anabaenopeptins, it should occur on the condensation domain (of the *N*-carboxy-L-amino acid, the donor substrate, and L-Lys, the acceptor substrate) possibly with the aid of the donor pantetheinyl arm (PPE) and the catalytic triad of the acceptor condensation domain. The catalysis might prevent the racemization of the donor amino acid prior to the hydantoin opening and explain the L-configuration of the starter amino acid in the anabaenopeptin despite the tendency of the immature hydantoanabaenopeptins, **1**–**4** and **6**, to racemize [28]. A biosynthetic route to the anabaenopeptins that encompass a mechanism similar to the one proposed for the ureido bridge formation in syringolin A is less feasible due to the occurrence, in the anabaenopeptin gene cluster, of two distinct adenylation and condensation domains for the amino acids involved in the construction of the ureido bridge production, unlike the single one for the syringolins [29]. The involvement of the epimerization domain in conversion of the hydantoin moiety to the mature anabaenopeptin is possible as well [30]. However, in the case of a presynthesized *N*-carboxy-amino acid loading to the first adenylation domain and its linking to the thiol through the *N*-carboxy moiety, one cannot exclude a direct biosynthesis of the ureido bridge. In such a case, the *N*-carboxy moiety might be phosphorylated (activated) and transferred to the thiol of the condensation domain and condensed with the amine of Lys to produce the ureido moiety

in one biosynthetic step. Iso-linked amino acids are known in cyanobacterial peptides, i.e., the iso-linked Glu, Asp and MeAsp in the microcystins [31]. Further biosynthetic studies, which are beyond our scientific skills, are required in order to conclude on this issue.

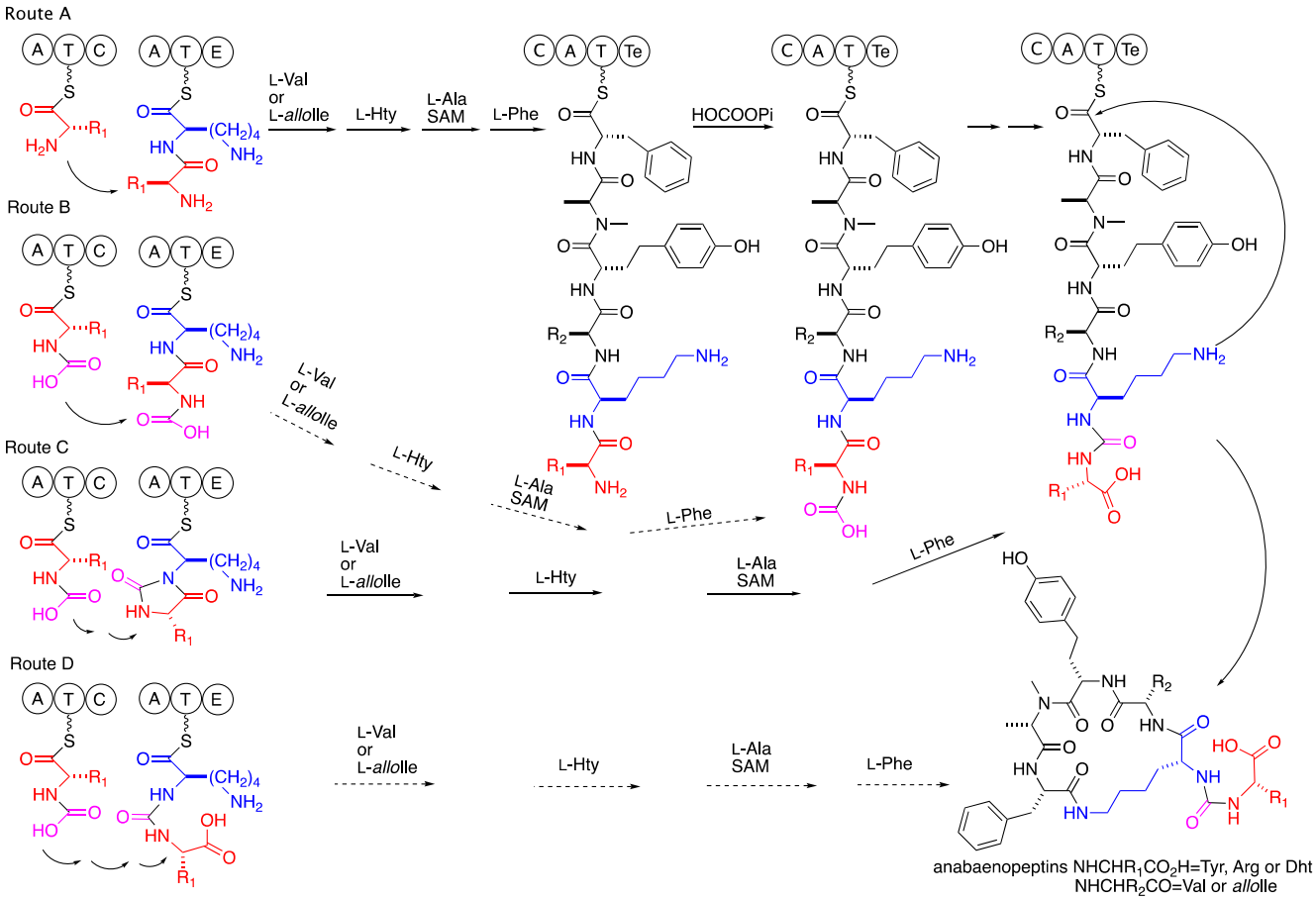

Scheme 2. Possible routes to the ureido bridge of the anabaenopeptins.

3. Material and Methods

3.1. General Experimental Procedure

Optical rotation values were obtained on a Jasco P-1010 polarimeter at the sodium D line (589 nm). UV spectra were recorded on an Agilent 8453 spectrophotometer (Agilent, Santa Clara, CA, USA). IR spectra were recorded on a Bruker Tensor 27 FT-IR instrument (Bruker, Billerica, MA, USA). NMR spectra were recorded on Bruker Avance III spectrometers (Bruker Karlsruhe, Germany) at 500.13 MHz for ^{1}H and 125.76 MHz for ^{13}C; chemical shifts were referenced to TMS δ_H and δ_C = 0 ppm. DEPT, COSY-45, gTOCSY, gROESY, gHSQC, and gHMBC spectra were recorded using standard Bruker pulse sequences. ESI low- and high-resolution mass spectra and MS/MS spectra were recorded on a Waters (Waters, Milford, MA, USA) Xevo G2-XS QTOP instrument equipped with Acquity Hi Class UPLC (binary solvent manager) with an FTN sample manager, column manager, and PDA detector, using a 2.1 × 50 mm BEH C18 (1.7 mm) column and a flow of 0.1–0.3 mL/min. HPLC separations were performed on an Agilent 1100 Series HPLC system (Agilent, Santa Clara, CA, USA).

3.2. Biological Material

Microcystis biomass, TAU collection number IL-444, was collected in February 2016 from Lake Kinneret, Israel. The cell mass was frozen and lyophilized. A sample of the cyanobacteria is deposited at the culture collection of Tel Aviv University.

3.3. Isolation Procedure

The freeze-dried cell mass (515 g) was extracted with 7:3 MeOH:H_2O (3 × 4 L). The solvent was evaporated to dryness to furnish the crude extract (45 g). Aliquots of the extract were fractionated (10 g in each separation) on an octadecyl-silica flash column (YMC-GEL, ODS, 120A, 4.4 × 6.4 cm), with an increasing concentration of MeOH in H_2O. The anabaenopeptins were eluted from the column with 8:2 MeOH:H_2O (fraction 9, 1 g). The latter fraction (A9, 1 g) was separated on a CombiFlash EZ C-18 column (Teledyne ISCO, 15.5 gr HP C18, 250 mg loaded in each separation) using linear gradient conditions from 95% H_2O to 100% MeCN (at a rate of 1% MeCN/min and a flow of 7 mL/min), resulting in 15 fractions. The fractions were analyzed by NMR and MS and merged into final 10 fractions (B1–B10). Selected fractions from the above were dissolved (20:80 MeCN:H_2O) and separated on a semipreparative HPLC RP-18 column (YMCPack ODS-AQ, 10 μm, 250 × 20 mm). Fraction B5 (72 mg) was separated under gradient conditions, from 4:1 to 1:1, 0.05% aqueous formic acid/MeCN, at a rate of 0.4% MeCN/min and a flow of 3 mL/min, to yield the known anabaenopeptin B (**8**, 2.1 mg, R_t 29.7 min, 4.1 × 10^{-4} % yield from dry cell weight) and the known oscillamide Y (**10**, 3.3 mg, R_t 52.4 min, 6.4 × 10^{-4} % yield). Fraction B6 (65 mg) was separated under gradient conditions, from 4:1 to 2:3, 0.05% aqueous formic acid/MeCN, at a rate of 0.3% MeCN/min and a flow of 2.5 mL/min, to yield the known anabaenopeptin F (**9**, 1.5 mg, R_t 40.6 min, 2.9 × 10^{-4}% yield) as well as the known anabaenopeptin A (**7**, 2.6 mg, R_t 63.1 min, 5.0 × 10^{-4}% yield). Fraction B7 (55 mg) was separated under gradient conditions, from 3:1 to 2:3, 0.05% aqueous formic acid/MeCN, at a rate of 0.3% MeCN/min and a flow of 2 mL/min, to yield the novel hydantoanabaenopeptin B (**2**, 2.2 mg, R_t 22.2 min, 4.3 × 10^{-4}% yield), the novel hydantoanabaenopeptin F (**3**, 1.5 mg, R_t 30.3 min, 2.9 × 10^{-4}% yield), and the novel ^{1}[Dht]-anabaenopeptin A (**5**, 1.2 mg, R_t 56.8 min, 2.3 × 10^{-4}% yield). Fraction B8 (43 mg) was separated under isocratic conditions, 1:3 0.05% aqueous formic acid/MeCN, at a flow of 2 mL/min, to yield the novel hydantoanabaenopeptin A (**1**, 2.1 mg, R_t 46.9 min, 4.1 × 10^{-4}% yield). Fraction B9 (37 mg) eluted with isocratic system conditions 36:64 0.05% aqueous formic acid/MeCN, at a flow of 2 mL/min, to yield both the novel hydanto-oscillamide Y (**4**, 1.4 mg, R_t 54.1 min, 2.7 × 10^{-4}% yield) and the novel ^{1}[Dht]-hydantoanabaenopeptin A (**6**, 0.9 mg, R_t 71.1 min, 1.7 × 10^{-4}% yield).

3.4. Physical Data of the Compounds

Hydantoanabaenopeptin A (**1**): $[a]_D^{22}$-14.0 (c 0.0019, MeOH); UV (MeOH); λ_{max} (log ε) 202 (4.05), 222 (3.79), 277 (2.93) nm; IR (ATR Diamond) n_{max} 3274, 2929, 2854, 1766, 1710, 1640, 1592, 1438, 1366 cm^{-1}; for ^{1}H and ^{13}C NMR data, see Table S1 in Supporting Information; HRESIMS $[M–H]^-$, *m*/*z* 824.3985 (calc for $C_{44}H_{54}N_7O_9$, 824.3983).

Hydantoanabaenopeptin B (**2**): $[\alpha]_D^{20}$-18.7 (c 0.0009, MeOH); UV (MeOH) λ_{max} (log ε) 202 (4.05), 220 (3.64), 277 (2.47) nm; IR (ATR Diamond) n_{max} 3340, 2931, 2855, 1770, 1710, 1640, 1592, 1457,1432, 1367, 1095 cm^{-1}; for ^{1}H and ^{13}C NMR data, see Table S2 in Supporting Information; HRESIMS $[M–H]^-$, *m*/*z* 817.4367 (calc for $C_{41}H_{57}N_{10}O_8$, 817.4361).

Hydantoanabaenopeptin F (**3**): $[\alpha]_D^{20}$-18.6 (c 0.002, MeOH); UV (MeOH) λ_{max} (log ε) 202 (4.05), 222 (3.71), 277 (2.74) nm; IR (ATR Diamond) n_{max} 3327, 2933, 2810, 1772, 1708, 1670, 1609, 1351 cm^{-1}; for ^{1}H and ^{13}C NMR data, see Table S3 in Supporting Information; HRESIMS $[M–H]^-$, *m*/*z* 833.4690 (calc for $C_{44}H_{63}N_7O_9$, 833.4687).

Hydanto-oscillamide Y (**4**): $[\alpha]_D^{20}$-20.0 (c 0.0015, MeOH); UV (MeOH) λ_{max} (log ε) 202 (4.05), 224 (3.79), 277 (2.86) nm; IR (ATR Diamond) n_{max} 3295, 2928, 2857, 1768, 1710, 1644, 1595, 1456, 1425, 1367, 1245 cm^{-1}; for ^{1}H and ^{13}C NMR data, see Table S4 in Supporting Information; HRESIMS $[M–H]^-$, *m*/*z* 838.4143 (calc for $C_{45}H_{56}N_7O_9$, 838.4140).

^{1}[Dht]-Anabaenopeptin A (**5**): $[\alpha]_D^{22}$-15.3 (c 0.0016, MeOH); UV (MeOH) λ_{max} (log ε) 202 (4.05), 223 (4.03), 276 (3.22) nm; IR (ATR Diamond) n_{max} 3318, 2942, 2861, 1658, 1642, 1595, 1515, 1416, 1244 cm^{-1}; for ^{1}H and ^{13}C NMR data, see Table S5 in Supporting Information; HRESIMS $[M + H]^+$, *m*/*z* 872.4560 (calc for $C_{46}H_{624}N_7O_{10}$, 872.4558).

^{1}[Dht]-Hydantoanabaenopeptin A (**6**): $[\alpha]_D^{22}$-8.8 (c 0.0011, MeOH); UV (MeOH) λ_{max} (log ε) 202 (4.05), 222 (3.91), 277 (3.03) nm; IR (ATR Diamond) n_{max} 3320, 2930, 2809,

1771, 1710, 1667, 1610, 1352 cm^{-1}; for ^{1}H and ^{13}C NMR data, see Table S6 in Supporting Information; HRESIMS $[M + H]^+$, m/z 854.4464 (calc for $C_{46}H_{60}N_7O_9$, 854.4453).

3.5. Determination of the Absolute Configuration of the Amino Acids by Marfey's Method [15]

Compounds **1**–**6** and authentic samples of anabaenopeptins A (**7**), B (**8**) and F (**9**) and oscillamide Y (**10**) were hydrolyzed in 6 N HCl (1 mL). The reaction mixture was maintained in a sealed glass bomb at 104 °C for 18 h. The acid was removed in vacuo, and the residue was suspended in 250 µL of H_2O. A solution of 1-fluoro-2,4-dinitrophenyl-5-L-alanine amide (FDAA) in acetone (0.03 M, 20 µL per each amino acid in the peptide) and $NaHCO_3$ (1 M, 20 µL per each amino acid) was added to the reaction vessel. The reaction mixture was stirred at 40 °C for 2.5 h in the dark. HCl (2 M, 10 µL per each amino acid) was added to the reaction vessel, and the solution was evaporated in vacuo. The samples of L-FDAA derivatives were analyzed by ESI LC MS. The analysis was performed on a Waters (USA) Xevo G2-XS QTOP instrument equipped with Acquity Hi Class UPLC (binary solvent manager) with an FTN sample manager, column manager, and PDA detector, using a 2.1 × 50 mm BEH C18 (1.7 mm) column and a flow of 0.1–0.3 mL/min. The mobile phase compositions were (A) Water containing 0.1% formic acid and (B) MeCN containing 0.1% formic acid. The elution gradient was as follows: 1 min of 100% A, linear gradient to 30% B over 60 min, and then recycling by linear gradient to 50% B over 10 min and to 100% A over additional 5 min. Samples of 10 µL were injected, and the flow rate was 0.1–0.3 mL/min. The UV detector was set to 340 nm, and the mass spectrometer was operated in both negative and positive ion modes, scanning between 100 and 1000 mass units. The interpretation of the data was conducted after the run on both positive and negative ion modes using Waters MassLynx software (v.4.1).

3.6. Protease Inhibition Assays

The samples for biological assays were dissolved in DMSO at a concentration of 1 mg/mL and were tested for inhibition of the proteases at a single concentration: **1** (55.1 mM), **2** (55.6 mM), **3** (54.6 mM), 4 (54.2 mM), **5** (53.3 mM), and **6** (53.3 mM). Assays were performed in a 96-well plate format.

3.6.1. Trypsin

The assay was performed in a Tris buffer (0.6 g Tris HCl in 100 mL H_2O, pH 7.5). Benzoyl-L-arginine-*p*-nitroanilide hydrochloride (BAPNA), the trypsin substrate, was dissolved at 1 mg/mL in 1:9 DMSO/buffer. The enzyme was dissolved in buffer at 1 mg/mL. To each well were added 100 µL of buffer, 10 µL of enzyme, and 10 µL of sample. The plate was placed in the spectrophotometer at 37 °C. After 5 min, 100 µL of substrate solution was added to each well, and the plate was placed in the spectrophotometer for the kinetic measurement of the absorbance intensity over 30 min at a wavelength of 405 nm.

3.6.2. Chymotrypsin

The assay was performed in a Tris buffer (0.6 gr TRIS HCl/100 mL H_2O, pH 7.5). The enzyme and the substrate Suc-Gly-Gly-phenylalanine-*p*-nitroanilide (SGGPNA) were dissolved in the buffer at a concentration of 1 mg/mL. To each well were added 100 µL of buffer, 10 µL of enzyme, and 10 µL of sample. Then, the plate was placed in the spectrophotometer for a 5 min incubation at 37 °C. Thereafter, to each well, 100 µL of substrate solution was added, and the plate was placed in the spectrophotometer for the kinetic measurement of the absorbance intensity over 30 min at a wavelength of 405 nm.

4. Conclusions

We are monitoring the seasonal blooms of cyanobacteria in Lake Kinneret for almost three decades [32–34]. Along the years, the spring *Microcystis* bloom was shifted from green to brown in color (dominant by the *Microcystis aeruginosa* strain marked Mic B due to its dominant pigmentation, brown color) [10,11]. The brown bloom material contains a large

amount of the aeruginosins KT608A and KT608B, which we use for an ongoing study on their ecological role. While isolating the aeruginosins for our study, we noticed several unknown masses in the LCMS of some fractions. The latter masses turned to be the new hydantoanabaenopeptins described above. The occurrence of hydantoanabaenopeptins may explain how the hexapeptide, encoded in the biosynthetic genes responsible for the biosynthesis of the anabaenopeptins in cyanobacteria, is converted to the ureido bridge containing anabaenopeptin. We propose several possible routes that include the formation and opening of the hydantoin moiety to the mature anabaenopeptin. The accumulation of the hydantoanabaenopeptins in this bloom material and the fact that it was not noticed in other studies in the past might result from the misfunction of the enzyme responsible for the production and opening of the hydantoin moiety, or misfunction of one of the enzymes that produces the hydantoin, as a by-product. Further genetic and enzymatic studies, which are beyond our capabilities, are needed to clarify this issue.

Supplementary Materials: The following supporting information can be downloaded at https://www.mdpi.com/article/10.3390/md21070401/s1; Figure S1: 1H NMR Spectrum of Hydanto-anabaenopeptin A (**1**) in DMSO-d6; Figure S2: 13C NMR Spectrum of Hydanto-anabaenopeptin A (**1**) in DMSO-d6; Figure S3: HSQC Spectrum of Hydanto-anabaenopeptin A (**1**) in DMSO-d6; Figure S4: HMBC Spectrum of Hydanto-anabaenopeptin A (**1**) in DMSO-d6; Figure S5: COSY Spectrum of Hydanto-anabaenopeptin A (**1**) in DMSO-d6; Figure S6: TOCSY Spectrum of Hydanto-anabaenopeptin A (**1**) in DMSO-d6; Figure S7: ROESY Spectrum of Hydanto-anabaenopeptin A (**1**) in DMSO-d6; Figure S8: Negative HR ESI MS of Hydanto-anabaenopeptin A (**1**); Figure S9: Positive HR ESI MS/MS Spectrum of Hydanto-anabaenopeptin A (**1**); Figure S10: Scheme of Fragmentation in the Positive HR ESI MS/MS Spectrum of Hydanto-anabaenopeptin A (**1**); Figure S11: LCMS Traces of Marfey's Method Amino Acids Analysis of Hydanto-anabaenopeptin A (**1**); Table S1: NMR Data of Hydanto-anabaenopeptin A (**1**) in DMSO-d6; Figure S12: LCMS Chromatogram and Mass spectrum of Hydanto-anabaenopeptin A (**1**); Figure S13: 1H NMR Spectrum of Hydanto-anabaenopeptin B (**2**) in DMSO-d6; Figure S14: 13C NMR Spectrum of Hydanto-anabaenopeptin B (**2**) in DMSO-d6; Figure S15: HSQC Spectrum of Hydanto-anabaenopeptin B (**2**) in DMSO-d6; Figure S16: HMBC Spectrum of Hydanto-anabaenopeptin B (**2**) in DMSO-d6; Figure S17: COSY Spectrum of Hydanto-anabaenopeptin B (**2**) in DMSO-d6; Figure S18: TOCSY Spectrum of Hydanto-anabaenopeptin B (**2**) in DMSO-d6; Figure S19: ROESY Spectrum of Hydanto-anabaenopeptin B (**2**) in DMSO-d6; Figure S20: Negative HR ESI MS of Hydanto-anabaenopeptin B (**2**); Figure S21: Positive HR ESI MS/MS Spectrum of Hydanto-anabaenopeptin B (**2**); Figure S22: Scheme of Fragmentation in the Positive HR ESI MS/MS Spectrum of Hydanto-anabaenopeptin B (**2**); Figure S23: LCMS Traces of Marfey's Method Amino Acids Analysis of Hydanto-anabaenopeptin B (**2**); Table S2: NMR Data of Hydanto-anabaenopeptin B (**2**) in DMSO-d6; Figure S24: LCMS Chromatogram and Mass spectrum of Hydanto-anabaenopeptin B (**2**); Figure S25: 1H NMR Spectrum of Hydanto-anabaenopeptin F (**3**) in DMSO-d6; Figure S26: 13C NMR Spectrum of Hydanto-anabaenopeptin F (**3**) in DMSO-d6 3; Figure S27: HSQC Spectrum of Hydanto-anabaenopeptin F (**3**) in DMSO-d6; Figure S28: HMBC Spectrum of Hydanto-anabaenopeptin F (**3**) in DMSO-d6; Figure S29: COSY Spectrum of Hydanto-anabaenopeptin F (**3**) in DMSO-d6; Figure S30: TOCSY Spectrum of Hydanto-anabaenopeptin F (**3**) in DMSO-d6; Figure S31: ROESY Spectrum of Hydanto-anabaenopeptin F (**3**) in DMSO-d6; Figure S32: Negative HR ESI MS of Hydanto-anabaenopeptin F (**3**); Figure S33. Positive HR ESI MS/MS Spectrum of Hydanto-anabaenopeptin F (**3**); Figure S34. Scheme of Fragmentation in the Positive HR ESI MS/MS Spectrum of Hydanto-anabaenopeptin F (**3**); Figure S35. LCMS Traces of Marfey's Method Amino Acids Analysis of Hydanto-anabaenopeptin F (**3**); Table S3. NMR Data of Hydanto-anabaenopeptin F (**3**) in DMSO-d6; Figure S36. LCMS Chromatogram and Mass spectrum of Hydanto-anabaenopeptin F (**3**); Figure S37. 1H NMR Spectrum of Hydanto-oscillamide Y (**4**) in DMSO-d6; Figure S38. 13C NMR Spectrum of Hydanto-oscillamide Y (**4**) in DMSO-d6; Figure S39. HSQC Spectrum of Hydanto-oscillamide n Y (**4**) in DMSO-d6; Figure S40. HMBC Spectrum of Hydanto-oscillamide Y (**4**) in DMSO-d6; Figure S41. COSY Spectrum of Hydanto-oscillamide Y (**4**) in DMSO-d6; Figure S42. TOCSY Spectrum of Hydanto-oscillamide Y (**4**) in DMSO-d6; Figure S43. ROESY Spectrum of Hydanto-oscillamide Y (**4**) in DMSO-d6; Figure S44. Negative HR ESI MS of Hydanto-oscillamide Y (**4**); Figure S45. Positive HR ESI MS/MS Spectrum of Hydanto-oscillamide Y (**4**); Figure S46. Scheme of Fragmentation in the Positive HR ESI MS/MS Spectrum of Hydanto-oscillamide Y (**4**) Figure S47. LCMS Traces of

Marfey's Method Amino Acids Analysis of Hydanto-oscillamide Y (**4**); Table S4. NMR Data of Hydanto-oscillamide Y (**4**) in DMSO-d6; Figure S48. LCMS Chromatogram and Mass spectrum of Hydanto-oscillamide Y (**4**); Figure S49. 1H NMR Spectrum of ^{1}[Dht]-Anabaenopeptin A (**5**) in DMSO-d6; Figure S50. 13C NMR Spectrum of ^{1}[Dht]-Anabaenopeptin A (**5**) in DMSO-d6; Figure S51. HSQC Spectrum of ^{1}[Dht]-Anabaenopeptin A (**5**) in DMSO-d6; Figure S52. HMBC Spectrum of ^{1}[Dht]-Anabaenopeptin A (**5**) in DMSO-d6; Figure S53. COSY Spectrum of ^{1}[Dht]-Anabaenopeptin A (**5**) in DMSO-d6; Figure S54. TOCSY Spectrum of ^{1}[Dht]-Anabaenopeptin A (**5**) in DMSO-d6; Figure S55. ROESY Spectrum of ^{1}[Dht]-Anabaenopeptin A (**5**) in DMSO-d6; Figure S56. Positive HR ESI MS of ^{1}[Dht]-Anabaenopeptin A (**5**) 4; Figure S57. Positive HR ESI MS/MS Spectrum of ^{1}[Dht]-Anabaenopeptin A (**5**); Figure S58. Scheme of Fragmentation in the Positive HR ESI MS/MS Spectrum of ^{1}[Dht]-Anabaenopeptin A (**5**); Figure S59. LCMS Traces of Marfey's Method Amino Acids Analysis of ^{1}[Dht]-Anabaenopeptin A (**5**); Table S5. NMR Data of ^{1}[Dht]-Anabaenopeptin A (**5**) in DMSO-d6; Figure S60. LCMS Chromatogram and Mass spectrum of ^{1}[Dht]-Anabaenopeptin A (**5**); Figure S61. 1H NMR Spectrum of Hydanto-^{1}[Dht]-anabaenopeptin A (**6**) in DMSO-d6; Figure S62. 13C NMR Spectrum of Hydanto-^{1}[Dht]-anabaenopeptin A (**6**) in DMSO-d6; Figure S63. HSQC Spectrum of Hydanto-^{1}[Dht]-anabaenopeptin A (**6**) in DMSO-d6; Figure S64. HMBC Spectrum of Hydanto-^{1}[Dht]-anabaenopeptin A (**6**) in DMSO-d6; Figure S65. COSY Spectrum of Hydanto-^{1}[Dht]-anabaenopeptin A (**6**) in DMSO-d6; Figure S66. TOCSY Spectrum of Hydanto-^{6}[Dht]-anabaenopeptin A (**6**) in DMSO-d6; Figure S67. ROESY Spectrum of Hydanto-^{1}[Dht]-anabaenopeptin A (**6**) in DMSO-d6; Figure S68. Positive HR ESI MS of Hydanto-^{1}[Dht]-anabaenopeptin A (**6**); Figure S69. Positive HR ESI MS/MS Spectrum of Hydanto-^{1}[Dht]-anabaenopeptin (**6**); Figure S70. Scheme of Fragmentation in the Positive HR ESI MS/MS Spectrum of Hydanto-^{1}[Dht]-anabaenopeptin (**6**); Figure S71. LCMS Traces of Marfey's Method Amino Acids Analysis of Hydanto-^{1}[Dht]-anabaenopeptin (**6**); Table S6. NMR Data of Hydanto-^{1}[Dht]-anabaenopeptin A (**6**) in DMSO-d6; Figure S72. LCMS Chromatogram and Mass spectrum of Hydanto-^{1}[Dht]-anabaenopeptin A (**6**); Figure S73. 1H NMR Spectrum of Anabaenopeptin A (**7**) in DMSO-d6; Figure S74. 13C NMR Spectrum of Anabaenopeptin A (**7**) in DMSO-d6; Figure S75. Negative HR ESI MS of Anabaenopeptin A (**7**); Figure S76. Positive HR ESI MS/MS Spectrum of Anabaenopeptin A (**7**); Figure S77. Scheme of Fragmentation in the Positive HR ESI MS/MS Spectrum of Anabaenopeptin A (**7**); Figure S78. LCMS Traces of Marfey's Method Amino Acids Analysis of Anabaenopeptin A (**7**); Figure S79. LCMS Chromatogram and Mass spectrum of Anabaenopeptin A (**7**); Figure S80. 1H NMR Spectrum of Anabaenopeptin B (**8**) in DMSO-d6; Figure S81. 13C NMR Spectrum of Anabaenopeptin B (**8**) in DMSO-d6; Figure S82. Positive HR ESI MS of Anabaenopeptin B (**8**); Figure S83. Positive HR ESI MS/MS Spectrum of Anabaenopeptin B (**8**) Figure S84. Scheme of Fragmentation in the Positive HR ESI MS/MS Spectrum of Anabaenopeptin B (**8**); Figure S85. LCMS Traces of Marfey's Method Amino Acids Analysis of Anabaenopeptin B (**8**); Figure S86. LCMS Chromatogram and Mass spectrum of Anabaenopeptin B (**8**) 5; Figure S87. ^{1}H NMR Spectrum of Anabaenopeptin F (**9**) in DMSO-d_6; Figure S88. Negative HR ESI MS of Anabaenopeptin F (**9**); Figure S89. Positive HR ESI MS/MS Spectrum of Anabaenopeptin F (**9**); Figure S90. Scheme of Fragmentation in the Positive HR ESI MS/MS Spectrum of Anabaenopeptin F (**9**); Figure S91. LCMS Traces of Marfey's Method Amino Acids Analysis of Anabaenopeptin F (**9**); Figure S92. LCMS Chromatogram and Mass spectrum of Anabaenopeptin F (**9**); Figure S93. 1H NMR Spectrum of Oscillamide Y (**10**) in DMSO-d6; Figure S94. Negative HR ESI MS of Oscillamide Y (**10**); Figure S95. Positive HR ESI MS/MS Spectrum of Oscillamide Y (**10**); Figure S96. Scheme of Fragmentation in the Positive HR ESI MS/MS Spectrum of Oscillamide Y (**10**); Figure S97. LCMS Traces of Marfey's Method Amino Acids Analysis of Oscillamide Y (**10**); Figure S98. LCMS Chromatogram and Mass spectrum of Oscillamide Y (**10**).

Author Contributions: Conceptualization, A.S. and S.C.; formal analysis, S.W.A.; investigation, S.W.A.; writing—original draft preparation, S.W.A.; writing—review and editing, S.C. and A.S.; supervision, S.C.; funding acquisition, S.C. All authors have read and agreed to the published version of the manuscript.

Funding: This research was funded by NSFC-ISF grant number 2628/16 and by ISF grant 1298/13 to S.C.

Acknowledgments: The authors thank N. Tal, from the Mass Spectrometry Facility of the School of Chemistry, for running the MS spectra. S.W.A. thanks the School of Chemistry for the partial financial support.

Conflicts of Interest: The authors declare no conflict of interest.

References

1. Monteiro, P.R.; Amaral, S.C.D.; Siqueira, A.S.; Xavier, L.P.; Santos, A.V. Anabaenopeptins: What We Know So Far. *Toxins* **2021**, *13*, 522. [CrossRef] [PubMed]
2. Zervou, S.-K.; Kaloudis, T.; Gkelis, S.; Hiskia, A.; Mazur-Marzec, H. Anabaenopeptins from Cyanobacteria in Freshwater Bodies of Greece. *Toxins* **2022**, *14*, 4. [CrossRef] [PubMed]
3. Rounge, T.B.; Rohrlack, T.; Nederbragt, A.J.; Kristensen, T.; Jakobsen, K.S. A genome-wide analysis of nonribosomal peptidesynthetase gene clusters and their peptides in a Planktothrix rubescens strain. *BMC Genom.* **2009**, *10*, 396. [CrossRef] [PubMed]
4. Shishido, T.K.; Jokela, J.; Fewer, D.P.; Wahlsten, M.; Fiore, M.F.; Sivonen, K. Simultaneous Production of Anabaenopeptins and Namalides by the Cyanobacterium *Nostoc* sp. CENA543. *ACS Chem. Biol.* **2017**, *12*, 2746–2755. [CrossRef] [PubMed]
5. Entfellner, E.; Frei, M.; Christiansen, G.; Deng, L.; Blom, J.; Kurmayer, R. Evolution of Anabaenopeptin Peptide Structural Variability in the Cyanobacterium Planktothrix. *Front. Microbiol.* **2017**, *8*, 219. [CrossRef]
6. Lima, S.T.; Alvarenga, D.O.; Etchegaray, A.; Fewer, D.P.; Jokela, J.; Varani, A.M.; Sanz, M.; Dörr, F.A.; Pinto, E.; Sivonen, K.; et al. Genetic Organization of Anabaenopeptin and Spumigin Biosynthetic Gene Clusters in the Cyanobacterium *Sphaerospermopsis torques-reginae* ITEP-024. *ACS Chem. Biol.* **2017**, *12*, 769–778. [CrossRef]
7. Rouhiainen, L.; Jokela, J.; Fewer, D.P.; Urmann, M.; Sivonen, K. Two Alternative Starter Modules for the Non-Ribosomal Biosynthesis of Specific Anabaenopeptin Variants in Anabaena (Cyanobacteria). *Chem. Biol.* **2010**, *17*, 265–273. [CrossRef]
8. Christiansen, G.; Philmus, B.; Hemscheidt, T.; Kurmayer, R. Genetic Variation of Adenylation Domains of the Anabaenopeptin Synthesis Operon and Evolution of Substrate Promiscuity. *J. Bacteriol.* **2011**, *193*, 3822–3831. [CrossRef]
9. Kaljunen, H.; Schiefelbein, S.H.H.; Stummer, D.; Kozak, S.; Meijers, R.; Christiansen, G.; Rentmeister, A. Structural Elucidation of the Bispecificity of A Domains as a Basis for Activating Non-natural Amino Acids. *Angew. Chem. Int. Ed.* **2015**, *54*, 8833–8836. [CrossRef]
10. Ninio, S.; Lupu, A.; Viner-Mozzini, Y.; Zohary, T.; Sukenik, A. Multiannual variations in Microcystis bloom episodes—Temperature drives shift in species composition. *Harmful Algae* **2020**, *92*, 101710. [CrossRef]
11. Kaplan-Levy, R.N.; Alster-Gloukhovski, A.; Benyamini, Y.; Zohary, T. Lake Kinneret phytoplankton: Integrating classical and molecular taxonomy. *Hydrobiologia* **2016**, *764*, 283–302. [CrossRef]
12. Elliott, T.H.; Natarajan, P.N. Infared studies of hydantoin and its derivatives. *J. Pharm. Pharmacol.* **1967**, *19*, 209–216. [CrossRef]
13. Harada, K.I.; Fujii, K.; Shimada, T.; Suzuki, M.; Sano, H.; Adachi, K.; Carmichael, W.W. Two cyclic peptides, anabaenopeptins, a third group of bioactive compounds from the cyanobacterium Anabaena flos-aquae NRC 525-17. *Tetrahedron Lett.* **1995**, *36*, 1511–1514. [CrossRef]
14. Shin, H.J.; Matsuda, H.; Murakami, M.; Yamaguchi, K. Anabaenopeptins E and F, two new cyclic peptides from the cyanobacterium Oscillatoria agardhii (NIES-204). *J. Nat. Prod.* **1997**, *60*, 139–141. [CrossRef]
15. Fujii, K.; Ikai, Y.; Mayumi, T.; Oka, H.; Suzuki, M.; Harada, K.-I. A Nonempirical Method Using LC/MS for Determination of the Absolute Configuration of Constituent Amino Acids in a Peptide: Elucidation of Limitations of Marfey's Method and of Its Separation Mechanism. *Anal. Chem.* **1997**, *69*, 3346–3352. [CrossRef]
16. Faris, W.M.; Safi, Z.S. Theoretical Investigation of Tautomerism Stability of Hydantoin in the Gas Phase and in Solution. *Orient. J. Chem.* **2014**, *30*, 1045–1054. [CrossRef]
17. Williams, D.E.; Craig, M.; Holmes, C.F.B.; Anderson, R.J. Ferintoic Acids A and B, New Cyclic Hexpeptides from the Freshwater Cyanobacterium Microcystis aeruginosa. *J. Nat. Prod.* **1996**, *59*, 570–575. [CrossRef]
18. Zi, J.; Lantvit, D.D.; Swanson, S.M.; Orjala, J. Lyngbyaureidamides A and B, two anabaenopeptins from the cultured freshwater cyanobacterium Lyngbya sp. (SAG 36.91). *Phytochemistry* **2012**, *74*, 173–177. [CrossRef]
19. Reshef, V.; Carmeli, S. Schizopeptin 791, a New Anabaenopeptin-like Cyclic Peptide from the *Cyanobacterium Schizothrix* sp. *J. Nat. Prod.* **2002**, *65*, 1187–1189. [CrossRef]
20. Schmidt, E.W.; Harper, M.K.; Faulkner, D.J. Mozamides A and B, Cyclic Peptides from a Theonellid Sponge from Mozambique. *J. Nat. Prod.* **1997**, *60*, 779–782. [CrossRef]
21. Sano, T.; Kaya, K. Oscillamide Y, A chymotrypsin Inhibitor from Toxic *Oscillatoria agardhii*. *Tetrahedron Lett.* **1995**, *36*, 5933–5936. [CrossRef]
22. Koketsu, K.; Mitsuhashi, S.; Tabata, K. Identification of Homophenylalanine Biosynthetic Genes from the Cyanobacterium Nostoc punctiforme PCC73102 and Application to Its Microbial Production by Escherichia coli. *Appl. Environ. Microbiol.* **2013**, *79*, 2201–2208. [CrossRef] [PubMed]
23. Schreuder, H.; Liesum, A.; Lönze, P.; Stump, H.; Hoffmann, H.; Schiell, M.; Kurz, M.; Toti, L.; Bauer, A.; Kallus, C.; et al. Isolation, Co-Crystallization and Structure-Based Characterization of Anabaenopeptins as Highly Potent Inhibitors of Activated Thrombin Activatable Fibrinolysis Inhibitor (TAFIa). *Sci. Rep.* **2016**, *6*, 32958. [CrossRef] [PubMed]
24. Riba, M.; Kiss-Szikszai, A.; Gonda, S.; Boros, G.; Vitál, Z.; Borsodi, A.K.; Krett, G.; Borics, G.; Ujvárosi, A.Z.; Vasas, G. Microcystis Chemotype Diversity in the Alimentary Tract of Bigheaded Carp. *Toxins* **2019**, *11*, 288. [CrossRef] [PubMed]

25. Huang, Y.-H.; Yang, P.-C.; Lin, E.-S.; Ho, Y.-Y.; Peng, W.-F.; Lu, H.-P.; Huang, C.-C.; Huang, C.-Y. Crystal Structure of Allantoinase from *Escherichia coli* BL21: A Molecular Insight into a Role of the Active Site Loops in Catalysis. *Molecules* **2023**, *28*, 827. [CrossRef] [PubMed]
26. Cheon, Y.-H.; Kim, H.-S.; Han, K.-H.; Abendroth, J.; Niefind, K.; Schomburg, D.; Wang, J.; Kim, Y. Crystal Structure of d-Hydantoinase from *Bacillus stearothermophilus*: Insight into the Stereochemistry of Enantioselectivity. *Biochemistry* **2002**, *41*, 9410–9417. [CrossRef]
27. Sakaue, H.; Kinouchi, T.; Fujii, N.; Takata, T. Isomeric Replacement of a Single Aspartic Acid Induces a Marked Change in Protein Function: The Example of Ribonuclease A. *ACS Omega* **2017**, *2*, 260–267. [CrossRef]
28. Bloudoff, K.; Schmeing, T.M. Structural and functional aspects of the nonribosomal peptide synthetase condensation domain superfamily: Discovery, dissection and diversity. *Biochim. Biophys. Acta (BBA)—Proteins Proteom.* **2017**, *1865*, 1587–1604. [CrossRef]
29. Imker, H.J.; Walsh, C.T.; Wuest, W.M. SylC Catalyzes Ureido-Bond Formation During Biosynthesis of the Proteasome Inhibitor Syringolin A. *J. Am. Chem. Soc.* **2009**, *131*, 18263–18265. [CrossRef]
30. Walsh, C.T.; O'Brien, R.V.; Khosla, C. Nonproteinogenic Amino Acid Building Blocks for Nonribosomal Peptide and Hybrid Polyketide Scaffolds. *Angew. Chem. Int. Ed.* **2013**, *52*, 7098–7124. [CrossRef]
31. Meyer, S.; Kehr, J.-C.; Mainz, A.; Dehm, D.; Petras, D.; Süssmuth, R.D.; Dittmann, E. Biochemical Dissection of the Natural Diversification of Microcystin Provides Lessons for Synthetic Biology of NRPS. *Cell Chem. Biol.* **2016**, *23*, 462–471. [CrossRef]
32. Sukenik, A.; Rosin, C.; Porat, R.; Teltsch, B.; Banker, R.; Carmeli, S. Toxins from Cyanobacteria and Their Potential Impact on Water Quality of Lake Kinneret, Israel. *Isr. J. Plant Sci.* **1998**, *46*, 109–115. [CrossRef]
33. Beresovsky, D.; Hadas, O.; Livne, A.; Sukenik, A.; Kaplan, A.; Carmeli, S. Toxins and Biologically Active Secondary Metabolites of Microcystis sp. isolated from Lake Kinneret. *Isr. J. Chem.* **2006**, *46*, 79–87. [CrossRef]
34. Lifshitz, M.; Carmeli, S. Metabolites of a Microcystis aeruginosa bloom material from Lake Kinneret, Israel. *J. Nat. Prod.* **2012**, *75*, 209–219. [CrossRef]